

## Multilayer atom chips for versatile atom micromanipulation

M. Trinker,<sup>1</sup> S. Groth,<sup>2</sup> S. Haslinger,<sup>1</sup> S. Manz,<sup>1</sup> T. Betz,<sup>1</sup> S. Schneider,<sup>1</sup>  
I. Bar-Joseph,<sup>3</sup> T. Schumm,<sup>1,a)</sup> and J. Schmiedmayer<sup>1,2</sup>

<sup>1</sup>Atominstytut, Vienna University of Technology, 1020 Vienna, Austria

<sup>2</sup>Physikalisches Institut, Universität Heidelberg, 69120 Heidelberg, Germany

<sup>3</sup>Department of Condensed Matter Physics, Weizmann Institute of Science, Rehovot 76100, Israel

(Received 30 January 2008; accepted 27 March 2008; published online 24 June 2008)

We employ a combination of optical and electron-beam lithography to create an atom chip combining submicron wire structures with larger conventional wires on a single substrate. The multilayer fabrication enables crossed wire configurations, greatly enhancing the flexibility in designing potentials for ultracold quantum gases and Bose–Einstein condensates. Large current densities of  $>6 \times 10^7$  A/cm<sup>2</sup> and high voltages of up to 65 V across 0.3  $\mu\text{m}$  gaps are supported by even the smallest wire structures. We experimentally demonstrate the flexibility of the next generation atom chip by producing Bose–Einstein condensates in magnetic traps created by a combination of wires involving all different fabrication methods and structure sizes. © 2008 American Institute of Physics. [DOI: 10.1063/1.2945893]

Manipulation of neutral atoms close to microstructured surfaces has become a standard technique during recent years. So called *atom chips*<sup>1,2</sup> combine the ability to use ultracold atoms—a system well suited for precise quantum manipulation—and the technological capabilities of micro- and nanofabrication. Ample techniques have been developed to trap, cool, and detect neutral atoms in microtraps.<sup>2–5</sup> Robust quantum manipulation on the atom chip is available, both for internal atomic states<sup>6</sup> and the external degree of freedom.<sup>7</sup>

Present atom chips are single layer devices,<sup>8</sup> sometimes combined with other structures, either macroscopic<sup>9</sup> or built from a combination of chips fabricated on separate substrates,<sup>10,11</sup> limiting the freedom in designing the trapping and manipulation potentials. In this letter, we present the implementation of a multilayer atom chip (Fig. 1) combining standard millimeter scale wires for trapping and cooling with submicron structures for manipulation on the quantum level on one single substrate. Such a chip design offers the advantage of precise alignment of the structures given by the inherent precision of the fabrication and the drastically reduced spatial distance of the respective structures.

To implement vastly different structure sizes on a single chip, we use a combination of traditional optical ultraviolet (UV) lithography and electron-beam lithography. The design consists of a standardized wire pattern (fabricated by UV lithography) which provides the backbone of the atom chip with all the connections and auxiliary wires needed for trapping, cooling, and positioning the ultracold atoms (Fig. 2, left). This general structure is complemented by an e-beam written part which can be custom designed for each chip realization individually (Fig. 2, right), offering high flexibility. A third pattern created by UV lithography above the e-beam layer adds chip wires to transport the atoms toward the e-beam structures and provides additional functionality.

The main requirements for such an atom chip are the ability to carry sizable currents of a few amps in the large structures to create deep traps, high current densities in the small structures for tight confinement,<sup>2,3</sup> to allow the appli-

cation of radio-frequency (rf) fields<sup>7,12</sup> and the capability to tolerate sizable voltages over submicron gaps to enable localized manipulation by electric fields.<sup>13</sup> To achieve this, one needs a perfectly electrically insulating layer with the capability of sufficient heat transfer from the upper wires to the substrate, which also withstands high electric fields. In our chip design, we achieve this by separating the different conducting layers by an electrically insulating thin (500 nm) polyimide layer. Conducting structures are fabricated by thermally evaporating gold layers (thicknesses from 130 nm to 4  $\mu\text{m}$ ), which provides the best achievable wire quality together with optimal optical reflection.<sup>14</sup>

Our atom chips are fabricated on commercial 700  $\mu\text{m}$  thick *p*-type Si wafers with a 100 nm thermal oxide layer for electrical isolation.<sup>8</sup> We start by depositing alignment marks which allow to superimpose the different layers with submicron precision. We then fabricate the submicron structures in the center  $600 \times 600 \mu\text{m}^2$  of the chip (Fig. 2, right). A double-layer polymethyl methacrylate (PMMA) resist (PMMA 495 and 950 K) is structured by e-beam lithography followed by depositing first a Ti adhesion layer (10 nm) and then the Au layer (130 nm), both by thermal evaporation at a

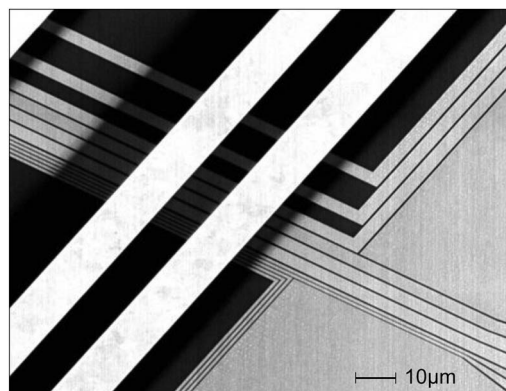


FIG. 1. SEM micrograph of the central part of a multilayer chip. 10  $\mu\text{m}$  wide wires with a height of 1.4  $\mu\text{m}$  cross structures created by e-beam lithography. The smallest features are 300 nm gaps between 700 nm wide and 140 nm high wires. Electrical insulation of the two layers is provided by 500 nm thick polyimide pads, visible as partially transparent layer.

<sup>a)</sup>Electronic mail: schumm@atomchip.org.

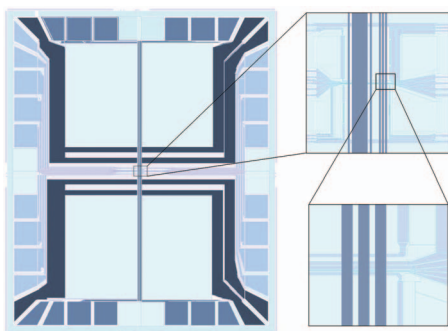


FIG. 2. (Color) Layout of a multilayer atom chip. Left: General view of the chip, size  $25 \times 30$  mm. Contact pads are arranged around the edge of the chip. Wires for trapping of atoms run from top to bottom (blue) on the upmost layer of the chip. Where these wires cross structures on the ground plane, polyimide pads provide insulation of the layers. For longitudinal confinement of the atoms, the chip contains four additional  $500 \mu\text{m}$  wide wires (dark blue) on the ground plane. Upper right: Central part of the chip ( $600 \times 600 \mu\text{m}^2$ ), created by e-beam lithography. Lower right: Detail of this central section ( $100 \times 100 \mu\text{m}^2$ ), similar to the region shown in Fig. 1. Three  $10 \mu\text{m}$  wide wires (blue) cross submicron structures (light blue, smallest features:  $300 \text{ nm}$  wide gaps) separated by polyimide pads.

pressure of  $10^{-7}$  mbar. Lift off in acetone supported by ultrasound then completes fabrication of the inner submicron structures of the chip.

In the next step, the connections to this central part, the pads for contacting the chip, and all other larger support structures are fabricated. We therefore employ our standard process for high quality atom chip structures.<sup>8</sup> The image reversal resist AZ5214E is structured by traditional UV contact lithography followed by thermal evaporation of Ti ( $20 \text{ nm}$ ) and Au ( $400 \text{ nm}$  in this specific example). The structures are created again by lift off in acetone.

We then prepare the insulation which will support the crossing structures. Polyimide [Durimide (R) 7505] is spun onto the chip and structured by UV lithography to cover only the regions where conducting structures will cross. The insulation layer is then thinned in an ozonator to about  $500 \text{ nm}$  and cured. This layer thickness proved to be sufficient to insulate the two conducting planes while providing good heat transfer and keeping the step height the top layer wires have to surmount to a minimum (Fig. 3).

The wires in the upper plane crossing the polyimide insulation pads are fabricated by UV-lithography.<sup>8</sup> To enable high currents in these wires, they can be evaporated to a height of up to  $4 \mu\text{m}$ . This also reduces the bottleneck created by the step onto the polyimide pads (Fig. 3).

The current characteristics of the various atom chip wires are tested by a four-point measurement, monitoring heating via resistance increase with time. The cold resistance of the structures ranges from  $100$  to  $300 \Omega$  for e-beam-written wires, and  $4.5$  to  $40 \Omega$  for the larger structures. Similar to the situation in the actual atom chip experiments, the measurements were carried out in a pulsed manner with a  $10 \text{ s}$  relaxation time.

For surface mounted wires, the results are similar to what was found in our previous study on single layer atom chips.<sup>8</sup> The heating process shows two different time scales: wires first heat up on a fast time scale ( $100 \text{ ns} - 1 \mu\text{s}$ ) after switching on the current, leading to a corresponding increase in wire resistance. On a longer timescale, a slow heating process is observed over the full duration of the current pulse

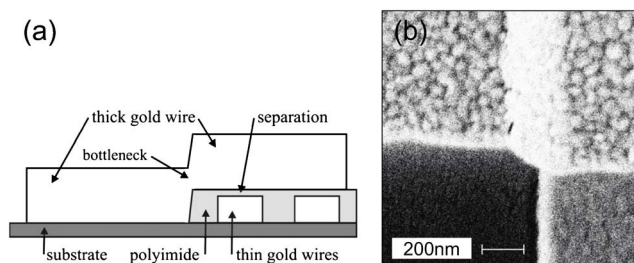


FIG. 3. (a) Cross section scheme of a multilayer area (not to scale). The step in the upper gold wire causes a bottleneck of reduced cross section. (b) SEM top view of the step. The wire runs from left to right in the upper half of the picture. In the lower right part, the polyimide pad running from top to bottom is visible.

(Fig. 4). In accordance with the model from Ref. 8, the highest current densities were tolerated by the wires of smallest cross section, see Fig. 4. A  $700 \text{ nm}$  wide and  $140 \text{ nm}$  high wire carried currents of up to  $60 \text{ mA}$  over a maximum of  $10 \text{ s}$ , corresponding to a current density of  $6 \times 10^7 \text{ A/cm}^2$ .

For the wires crossing the polyimide insulation pads, we observe a similar behavior with a reduced maximal current due to the decreased thermal conductivity to the substrate. Nevertheless large current densities of above  $3 \times 10^6 \text{ A/cm}^2$  ( $2 \times 10^6 \text{ A/cm}^2$ ) can be supported by a  $10 \mu\text{m}$  ( $80 \mu\text{m}$ ) wide wire (Fig. 4). dc currents of up to  $2.3 \text{ A}$  are sustained by the  $80 \mu\text{m}$  wide and  $1.4 \mu\text{m}$  high wire.

A crucial test for the double-layer chip structures is to which extend a current or voltage in the wires in the bottom layer influences the current limits in the wires above. We study this by measuring the temperature evolution of a  $80 \mu\text{m}$  top layer wire after switching on additional  $500 \mu\text{m}$  wide,  $400 \text{ nm}$  high confinement wires in the ground plane. A clear increase in resistance and hence heating of the top wires depending on the current density in the lower wires can be observed (Fig. 4). For the largest currents in the bottom wires, the maximum current sustained in the top wires can be reduced by a factor of 2.

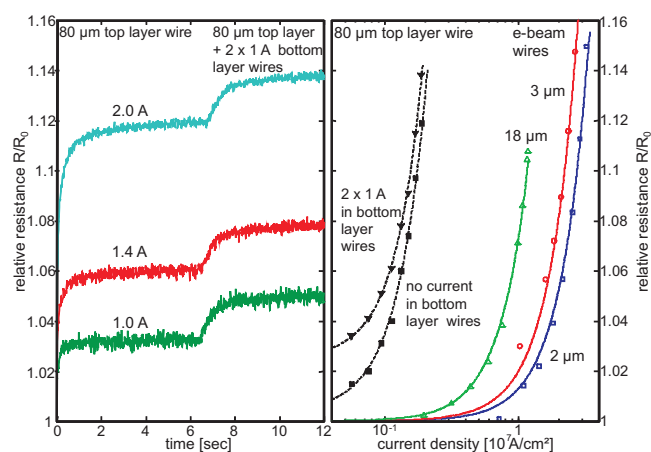


FIG. 4. (Color) Left: Temperature evolution of a  $80 \mu\text{m}$  top layer trapping wire for different applied currents. After  $\approx 6 \text{ s}$ , an additional current of  $1 \text{ A}$  is sent through two  $500 \mu\text{m}$  bottom layer confinement wires, as in the experiment shown in Fig. 5. Right: Temperature evolution for different current densities in various chip wires. Solid lines are theoretical predictions according to a simple dissipation model which applies to bottom layer e-beam wires in direct contact with the substrate (Ref. 8). Reduced heat dissipation reduces the current density for top layer wires, currents in the bottom layer wires lead to additional heating (dashed lines to guide the eye).

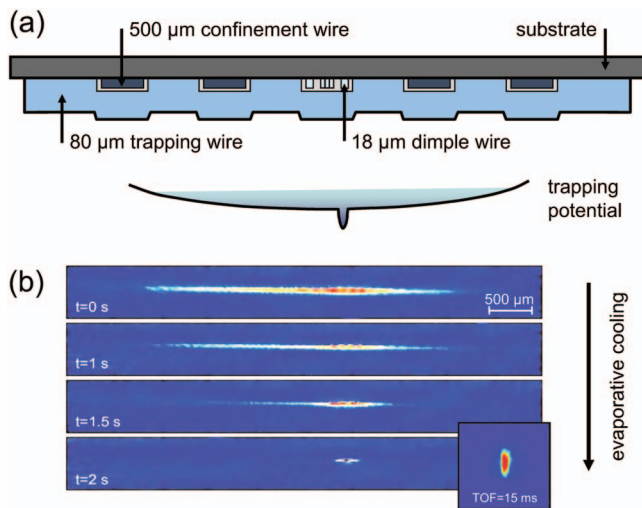


FIG. 5. (Color) (a) Magnetic trapping potential created by the combined fields of the outer  $500\ \mu\text{m}$  bottom layer confinement wires (dark blue), the main  $80\ \mu\text{m}$  top layer trapping wire (blue), and a  $10\ \mu\text{m}$  e-beam fabricated dimple wire (light blue), creating a local potential minimum. (b) *In situ* absorption images of an atom cloud, evaporatively cooled in the combined potential. Inset: time-of-flight (TOF) absorption image after 15 ms free expansion, clearly indicating Bose–Einstein condensation.

The combination of submicron wires connected to larger structures causes nonuniform heat dissipation and can lead to delicate failure modes. The resistivity change is not a firm indication any more, as it was in the single layer chips.<sup>8</sup> The different parts of the wire contribute differently (locally) to heating, and a simple rule of how much resistivity increase can safely be tolerated cannot be determined. Hence, current limits have to be found for each individual wire category. For example, the submicron wires in the central part tend to burn for an increase of  $R/R_0$  by more than 20%, whereas the larger wires in a single layer chip easily support an increase by 100%.

In voltage tests, even the smallest wire structures allowed to apply sizable voltages of  $>65\ \text{V}$  without breakdown. This allows to apply electric field of over  $200\ \text{kV/mm}$  over the  $300\ \text{nm}$  gaps between e-beam wires, creating extremely steep and localized potentials.<sup>13</sup>

Our multilayer atom chip combines many functionalities in a single device. The large top layer wires ( $10\text{--}80\ \mu\text{m}$  width,  $1.4\ \mu\text{m}$  height) can carry sizable currents of above  $2\ \text{A}$  to create the magnetic traps for trapping, cooling, and positioning ultracold atom clouds or Bose–Einstein condensates (BECs) together with strong rf oscillating fields for dressed-state potentials.<sup>7,12</sup> Large bottom layer confinement wires equally enable high currents and allow adjustment of trap aspect ratio over many orders of magnitudes. The small e-beam wires allow micron size structuring of the potentials for manipulation of the trapped atoms on a scale where tunneling and coupling between traps can be studied.

We experimentally demonstrate the double-layer atom chip flexibility by creating BECs of rubidium atoms in a magnetic trapping potential created by a combination of all structures described above [Fig. 5(a)]. Starting point is a re-

flexion magneto-optical trap, using the high quality gold surfaces of the atom chip as a mirror. Macroscopic copper wire structures below the chip create the magnetic fields necessary for laser cooling, initial magnetic trapping and transport to the atom chip.<sup>9</sup> Atoms are then loaded into a chip trap combining magnetic fields of a top layer  $80\ \mu\text{m}$  trapping wire and two  $500\ \mu\text{m}$  bottom layer confinement wires in series, each carrying  $1\ \text{A}$ . Sending  $40\ \text{mA}$  through a  $18\ \mu\text{m}$  bottom layer e-beam wire locally lowers the potential, creating an adjustable magnetic dimple.<sup>15</sup> Efficient and robust Bose condensation is achieved by forced rf evaporation in the combined trap, as shown in Fig. 5(b).

To summarize, we have presented fabrication, characterization, and implementation of an atom chip combining structures created with traditional UV and e-beam lithography in a multilayer geometry. With this concept, we integrated wires tolerating extreme current densities and electric fields with established structures for robust trapping of cold atoms in a single device. In addition, the influence of currents in the ground plane wires on the resistance of wires crossing these structures was analyzed. We experimentally demonstrate the atom chip flexibility by producing BECs in a potential involving all of the major wire structures.

We thank O. Raslin, Braun Center for Submicron Research at the Weizmann Institute of Science, for help in the fabrication. We also thank S. Hofferberth, S. Wildermuth, and P. Krüger for help in the conception and design of the atom chip. This work was supported by the European Union, Contract No. IST-2001-38863 (ACQP), Integrated Project FET/QIPC “SCALA,” the Austrian Science Fund FWF Project P20372.

<sup>1</sup>R. Folman, P. Krüger, and D. Cassettari *et al.*, *Phys. Rev. Lett.* **84**, 4749 (2000).

<sup>2</sup>J. Fortagh and C. Zimmermann, *Rev. Mod. Phys.* **79**, 235 (2007).

<sup>3</sup>R. Folman, P. Krüger, and J. Schmiedmayer *et al.*, *Adv. At., Mol., Opt. Phys.* **48**, 263 (2002).

<sup>4</sup>Y. Colombe, T. Steinmetz, and G. Dubois *et al.*, *Nature (London)* **450**, 272 (2007).

<sup>5</sup>X. Liu, K.-H. Brenner, and M. Wilzbach *et al.*, *Appl. Opt.* **44**, 6857 (2005).

<sup>6</sup>P. Treutlein, P. Hommelhoff, and T. Steinmetz *et al.*, *Phys. Rev. Lett.* **92**, 203005 (2004).

<sup>7</sup>T. Schumm, S. Hofferberth, and L. M. Andersson *et al.*, *Nat. Phys.* **1**, 57 (2005).

<sup>8</sup>S. Groth, P. Krüger, and S. Wildermuth *et al.*, *Appl. Phys. Lett.* **85**, 2980 (2004).

<sup>9</sup>S. Wildermuth, P. Krüger, and C. Becker *et al.*, *Phys. Rev. A* **69**, 030901(R) (2004).

<sup>10</sup>A. Günther, M. Kemmler, and S. Kraft *et al.*, *Phys. Rev. A* **71**, 063619 (2005).

<sup>11</sup>J. Esteve, T. Schumm, and J.-B. Trebbia *et al.*, *Eur. Phys. J. D* **35**, 141 (2005).

<sup>12</sup>S. Hofferberth, I. Lesanovsky, and B. Fischer *et al.*, *Nat. Phys.* **2**, 710 (2006).

<sup>13</sup>P. Krüger, X. Luo, and M. W. Klein *et al.*, *Phys. Rev. Lett.* **91**, 233201 (2003).

<sup>14</sup>P. Krüger, L. M. Andersson, and S. Wildermuth *et al.*, *Phys. Rev. A* **76**, 063621 (2007).

<sup>15</sup>D. M. Stamper-Kurn, H.-J. Miesner, and A. P. Chikkatur *et al.*, *Phys. Rev. Lett.* **81**, 2194 (1998).